

# The Equation of state for two flavor QCD at $N_t = 6$

**Claude Bernard**

*Department of Physics, Washington University, St. Louis, MO 63130, USA*

**Tom Blum**

*Department of Physics, Brookhaven National Lab, Upton, NY 11973, USA*

**Carleton DeTar**

*Physics Department, University of Utah, Salt Lake City, UT 84112, USA*

**Steven Gottlieb, Kari Rummukainen \***

*Department of Physics, Indiana University, Bloomington, IN 47405, USA*

**Urs M. Heller**

*SCRI, Florida State University, Tallahassee, FL 32306-4052, USA*

**James E. Hetrick<sup>†</sup>, Doug Toussaint**

*Department of Physics, University of Arizona, Tucson, AZ 85721, USA*

**Leo Kärkkäinen**

*Nokia Research Center, P.O. Box 100, FIN-33721 Tampere, Finland*

**Bob Sugar**

*Department of Physics, University of California, Santa Barbara, CA 93106, USA*

**Matthew Wingate**

*Physics Department, University of Colorado, Boulder, CO 80309, USA*

February 1, 2008

## Abstract

We calculate the two flavor equation of state for QCD on lattices with lattice spacing  $a = (6T)^{-1}$  and find that cutoff effects are substantially reduced compared to an earlier

---

\*new address: Fakultät für Physik, Universität Bielefeld, D-33615, Bielefeld, Germany

<sup>†</sup>new address: Department of Physics, Washington University, St. Louis, MO 63130, USA

study using  $a = (4T)^{-1}$ . However, it is likely that significant cutoff effects remain. We fit the lattice data to expected forms of the free energy density for a second order phase transition at zero-quark-mass, which allows us to extrapolate the equation of state to  $m_q = 0$  and to extract the speed of sound. We find that the equation of state depends weakly on the quark mass for small quark mass.

## 1 Introduction

It is generally believed that at high temperatures QCD undergoes either a phase transition or a fairly sharp crossover into a regime where hadrons “dissolve” into a quark-gluon plasma. Testing this scenario is a major goal of current and planned experiments in heavy ion collisions. Although the fireball created in such a collision is at best in quasi-equilibrium, knowledge of the equilibrium equation of state for QCD is nonetheless very useful for constraining the parameters of models of the quark-gluon plasma[1]. For this reason we have been carrying out a program of lattice simulations to determine this equation of state, or energy and pressure as a function of temperature. Our calculations include two degenerate quark flavors. However, the strange quark is neglected, and we work at zero net baryon density.

While the approximations made in a lattice simulation are controllable in principle, with presently available computing power these approximations are severe. In particular, effects of the nonzero lattice spacing are large. For example, there are big differences between the continuum Stefan-Boltzmann law, which is presumably the limit of the QCD energy at very high temperatures, and the lattice version, obtained by summing over the Fourier modes with the free particle action on the lattice. Also, with the Kogut-Susskind quarks that are usually used in high temperature QCD simulations, flavor symmetry (isospin symmetry, more or less) is badly broken. Instead of having  $N_f^2 - 1$  light pseudo-scalar particles at low temperature, only one pion is an exact Goldstone boson corresponding to a symmetry not broken by lattice artifacts. The breaking of flavor symmetry is expected to be proportional to  $a^2$  ( $a$  is the lattice spacing). It can be reduced by modifying the action[2] or by simply decreasing the lattice spacing.

In this work we report on an extension of our equation of state calculations to six time slices [3], which is a lattice spacing  $a = 1/(6T)$  instead of the  $a = 1/(4T)$  used in our earlier work [4]. In addition to decreasing the lattice spacing, we improve the extrapolation of our results to smaller quark mass by fitting our free energy to a form with either the theoretically predicted  $O(4)$  critical behavior or with the mean field behavior that is expected when we are not very close to the critical point.

## 2 Theory

The methods for computing the energy and pressure are standard[5, 6, 7], and we have discussed them in our earlier paper[4]. Here we summarize the equations necessary to make this paper self contained.

The energy, pressure and interaction measure are defined by

$$\begin{aligned}\varepsilon V &= -\frac{\partial \log Z}{\partial(1/T)} \\ \frac{p}{T} &= \frac{\partial \log Z}{\partial V} \\ I &= E - 3P = \frac{-T}{V} \frac{\partial \log(Z)}{\partial \log(a)}\end{aligned}\tag{1}$$

The temperature and volume are determined by the lattice spacing  $a$  and the space and time dimensions of the lattice,  $N_s$  and  $N_t$ .

$$\begin{aligned}V &= N_s^3 a^3, \\ 1/T &= N_t a \quad ,\end{aligned}\tag{2}$$

We use the  $1 \times 1$  plaquette (Wilson) action for the gauge fields, and the conventional Kogut-Susskind quark action with two flavors of quarks.

$$Z = \int [dU_{(n,\mu)}] \exp\{ (6/g^2) S_g + (n_f/4) \text{Tr} \log[am_q + \not{D}] \} \quad ,\tag{3}$$

$$S_g = \frac{1}{3} \text{Re} \sum_{n,\mu < \nu} \text{Tr} U_{\square}(n, \mu, \nu) \quad ,\tag{4}$$

In a lattice simulation we compute derivatives of the partition function. From these we can either explicitly or implicitly construct the partition function and from that the energy and pressure. In this work we make use of these quantities:

$$\langle \square \rangle = \frac{1}{2N_s^3 N_t} \frac{\partial \log(Z)}{\partial 6/g^2}\tag{5}$$

$$\langle \bar{\psi} \psi \rangle = \frac{1}{N_s^3 N_t} \frac{\partial \log(Z)}{\partial am_q}\tag{6}$$

$$\langle \square^2 \rangle - \langle \square \rangle^2 = \frac{1}{4N_s^3 N_t} \frac{\partial^2 \log(Z)}{\partial (6/g^2)^2}\tag{7}$$

$$\langle \square \bar{\psi} \psi \rangle - \langle \square \rangle \langle \bar{\psi} \psi \rangle = \frac{1}{2N_s^3 N_t} \frac{\partial^2 \log(Z)}{\partial am_q \partial 6/g^2}\tag{8}$$

The other second derivative of  $\log(Z)$ ,  $\partial^2 \log(Z) / \partial(am_q)^2$ , involves a disconnected piece which is not calculated here.

For large systems the free energy is proportional to the volume, and the pressure becomes just

$$p = \frac{T}{V} \log(Z) \quad (9)$$

Then derivatives of the free energy are just derivatives of the pressure, and the pressure can be reconstructed by integrating the free energy

$$\frac{pV}{T}(6/g^2, am_q) = 2N_s^3 N_t \int_{\text{cold}}^{6/g^2} [\langle \square(6/g^2, am_q) \rangle - \langle \square(6/g^2, am_q) \rangle_{\text{sym}}] d(6/g^2) \quad , \quad (10)$$

or

$$\frac{pV}{T}(6/g^2, am_q) = N_s^3 N_t \int_{\text{cold}}^{am_q} [\langle \bar{\psi}\psi(6/g^2, m'_q a) \rangle - \langle \bar{\psi}\psi(6/g^2, m'_q a) \rangle_{\text{sym}}] d(m'_q a) \quad , \quad (11)$$

where the “symmetric” quantities subtract the divergent zero-temperature pressure. The interaction measure can be found from simulations at a single value of  $(6/g^2, am_q)$  and the beta function, which tells how these lattice couplings must be changed to change the lattice spacing.

$$\frac{IV}{T} = -2N_s^3 N_t \frac{\partial(6/g^2)}{\partial \log a} [\langle \square \rangle - \langle \square \rangle_{\text{sym}}] - N_s^3 N_t \frac{\partial(am_q)}{\partial \log a} [\langle \bar{\psi}\psi \rangle - \langle \bar{\psi}\psi \rangle_{\text{sym}}] \quad (12)$$

In reference[4] we obtained the nonperturbative beta function for couplings associated with the  $N_t = 4$  and 6 crossovers. To briefly summarize, zero temperature spectrum data from the literature are combined in a fit which gives  $am_\pi$  and  $am_\rho$  as smooth functions of  $6/g^2$  and  $am_q$ . The  $\rho$  mass is used to define the lattice spacing. In particular, we somewhat arbitrarily set the  $\rho$  mass to 770 MeV at all light quark masses. Lines of constant physics (*i.e.*,  $m_\pi/m_\rho = \text{constant}$ ), along which the lattice spacing varies, are determined in the bare coupling space. The two components of the beta function,  $\partial(6/g^2)/\partial(\log a)$  and  $\partial(am_q)/\partial(\log a)$ , tell how the input parameters change along these lines of constant physics.

### 3 Simulations

For the equation of state, we have carried out simulations using the hybrid molecular dynamics  $R$  algorithm[8]. The calculation requires both asymmetric ( $12^3 \times 6$ ) and symmetric ( $12^4$ ) lattices as mentioned above. These are commonly referred to as hot and cold lattices, respectively, and we will use this terminology. This is somewhat misleading since the system may be in the cold phase, *i.e.* below the crossover, even on the hot lattices if the coupling

is small enough. Each hot (cold) simulation is at least 1800 (800) time units long after equilibration. As a rule, fewer trajectories were required for the "cold" lattices to achieve the same level of statistical accuracy because the lattice volume was twice as large. On the hot lattices near the crossover region the simulations were extended to more than 3000 units to overcome the larger fluctuations associated with the transition.

The bare coupling and quark mass phase diagram corresponding to our simulations is shown in Fig. 1. The vertical bars denote the approximate location of the finite temperature crossover for  $am_q = 0.0125$  and  $0.025$ . Note, while increasing the coupling  $6/g^2$  is analogous to increasing the temperature, lowering the bare quark mass  $am_q$  also increases the temperature. (This statement depends on the physical quantity used to define the lattice spacing. Again, we use  $m_\rho$ .) Of course there are lines in this bare coupling phase diagram on which  $m_\pi/m_\rho$  is fixed and only the physical temperature of the system varies. In particular, the bottom of the graph, where  $m_\pi/m_\rho = 0$ , is the line  $am_q = 0$  and corresponds approximately to the real world. In our simulations the gauge coupling  $6/g^2$  takes the values  $5.35 \leq 6/g^2 \leq 5.6$  for quark mass  $am_q = 0.0125$  and  $5.37 \leq 6/g^2 \leq 5.53$  for  $am_q = 0.025$ . Then along the line  $6/g^2 = 5.45$ , the quark mass varies in the range  $0.01 \leq am_q \leq 0.1$  and at  $6/g^2 = 5.53$ ,  $0.0125 \leq am_q \leq 0.2$ . This range of couplings and masses corresponds roughly to physical temperatures  $125 < T < 250$  MeV (based on the  $\rho$  mass[4]) and mass ratios  $0.3 < m_\pi/m_\rho < 0.7$ . In units of the pseudo-critical temperature  $T_c$ ,  $m_\pi/T_c = 1.94$  and  $2.69$  for  $am_q = 0.0125$  and  $0.025$ , respectively. Past lattice simulations indicate that  $T_c/m_\rho \approx 0.2$ [9], or  $m_\pi/T_c \approx 0.9$  in the continuum limit. Thus our simulations correspond to rather heavy pions.

The  $R$  algorithm introduces lowest order errors in observables that are proportional to  $\Delta t^2$ , where  $\Delta t$  is the step size used to numerically integrate the gauge field equations of motion through simulation time[8]. The errors are in general different on hot and cold lattices, thus multiple simulations at each value of  $6/g^2$  and  $am_q$  are required to extrapolate observables to  $\Delta t = 0$ [4]. Of course, this greatly increases the computational cost of the calculation since at each time step the force term due to the quarks in the gauge field equations of motion requires the inverse of the quark matrix, and as it happens,  $\Delta t$  must be taken relatively small ( $\simeq am_q$ ) to be in the regime where the lowest order error dominates. Thus many inversions of the quark matrix are required for each simulation. In Fig. 2 we show example results for the plaquette ( $\langle \square \rangle$ ) at  $am_q = 0.0125$ . Evidently, on the cold lattices and for lower values of  $6/g^2$ , the effects are worse. The step size errors are particularly troublesome for the plaquette since the difference of the plaquette on hot and cold lattices is quite small (even in the hot phase), as we will see in the next section. At low temperature both  $\langle \bar{\psi}\psi \rangle$  and  $\langle \square \rangle$  approach their symmetric values, making extraction of thermodynamic quantities in the hadronic phase very difficult.

## 4 Results and Analysis

The expectation values of  $\langle \square \rangle$  and  $\langle \bar{\psi}\psi \rangle$  are shown in Figs. 3 and 4. These values reflect the step size extrapolations. In each figure, a small but noticeable inflection point is observable in the expectation values on the hot lattices at  $6/g^2 \approx 5.415 (am_q = 0.0125)$  and  $5.445 (am_q = 0.025)$ . These couplings correspond to the pseudo-critical temperatures of the crossover. The expectation values are smooth on the cold lattices. Note that the values on the hot lattices approach their cold values at small  $6/g^2$  and begin to separate as  $6/g^2$  (and thus the temperature) is increased. The area between the curves in Fig. 3 yields  $p/T^4$ . At large  $6/g^2$ , the plaquette expectation values again approach each other since  $p/T^4 \rightarrow \text{constant}$  as  $T \rightarrow \infty$ , as expected from asymptotic freedom of QCD. The qualitative behavior of  $\langle \bar{\psi}\psi \rangle$  is consistent with its expected role as an order parameter for a spontaneously broken chiral symmetry. A quantitative analysis and extrapolation to zero-quark-mass is given later.

Next we turn to a discussion of the pressure. The integration of  $\langle \bar{\psi}\psi \rangle$  with respect to  $am_q$  at  $6/g^2 = 5.45$  and  $5.53$  yields the pressure as a function of  $am_q$  at fixed  $6/g^2$ , shown in Fig. 5. For large  $am_q$  the system is in the cold phase, and as  $am_q$  decreases, the pressure smoothly increases. To extrapolate the pressure from our smallest quark mass to zero-quark-mass requires a corresponding extrapolation of the cold and hot contributions to the integrand in (11). For the hot lattices at both values of  $6/g^2$  the extrapolation takes place in the hot phase, so for this contribution we assume  $\langle \bar{\psi}\psi \rangle = 0$  at  $am_q = 0$ . For the cold lattices we extrapolate using the fit summarized in Table 1. A simple linear extrapolation of the hot lattice data for the smallest two quark masses gives a result within  $1.5\sigma$  of zero at  $6/g^2 = 5.45$  and  $3.0\sigma$  of zero at  $6/g^2 = 5.53$ , perhaps due to curvature effects or underestimated errors. In any event forcing a zero intercept has a negligible effect on the pressure extrapolation.

As mentioned above, the pressure as a function of  $6/g^2$  at fixed quark mass is obtained by integrating  $\langle \square \rangle$  with respect to  $6/g^2$ . In Fig. 6 we show the results for  $am_q = 0.025$  and  $0.0125$ . Again, the pressure rises smoothly through the crossover. The curves are similar except for an overall shift in  $6/g^2$ , the  $am_q = 0.0125$  curve beginning its rise sooner since the smaller quark mass corresponds to higher temperature. Shown where they can be compared are the points obtained from the the quark mass integration. The values from the two different approaches agree, indicating that the integration method works well for the volumes studied.

The interaction measure at each point is just the sum of the  $T = 0$  subtracted values of the  $\langle \square \rangle$  and  $\langle \bar{\psi}\psi \rangle$  weighted by the coupling and quark mass components of the  $\beta$  function, respectively (Eq. 12). The results for  $am_q = 0.0125$  and  $0.025$  are shown in Fig. 7. At zero temperature the interaction measure is zero since we have normalized  $\varepsilon$  and  $p$  to be zero at  $T = 0$ . Through the transition, we expect  $I$  to increase rapidly if the energy density increases rapidly, *e.g.* if the quarks and gluons deconfine, since the pressure must rise smoothly (even

for a discontinuous transition) to maintain mechanical equilibrium of the system. This behavior is seen in Fig. 7. Again, at higher temperature due to asymptotic freedom, we expect  $I$  to decrease to zero as both the energy density and pressure asymptotically approach their Stefan-Boltzman values, and  $\varepsilon = 3p$ , the equation of state for a relativistic free gas.

The energy density constructed from  $I$  and  $p$  is shown in Fig. 8. Here we include  $3p$  as well. We also plot  $\varepsilon$  and  $3p$ , using the values of the  $\langle \square \rangle$  and  $\langle \bar{\psi}\psi \rangle$  at the smallest step size available at each point, without step size extrapolations. The difference between the two gives an estimate of the step size systematic error in our final results. Recall that step size effects for larger masses were essentially eliminated by taking  $\Delta t \ll am_q$ .

In Fig. 9 we show the equation of state as a function of the physical temperature. The quark mass dependence is largely removed by this partial rescaling,  $\{6/g^2(a), am_q(a)\} \rightarrow \{T(6/g^2, am_q), am_q\}$ . Note that the physical quark mass, or more precisely  $m_\pi/m_\rho$ , varies along each line of constant  $am_q$  while  $m_q/T = am_q N_t$  is held fixed. From the figure, we see a large increase in the energy density as  $T$  increases through the pseudo-critical temperature  $T_c \approx 140$  MeV ( $6/g_c^2$  was defined above). Just below  $T_c$ ,  $\varepsilon/T^4 \approx 5$  which is already substantial. Physically this means the hadronic phase has non-negligible energy density, except that it is not clear what degrees of freedom are being excited since we have already mentioned that  $m_\pi/T_c$  is roughly 2 to 3. A similar situation exists for the SU(3) pure gauge case where the ratio of the lightest glueball state to  $T_c$  is greater than 5[10]. We also note that the energy density of a relativistic gas of three light pions is insufficient to explain the observed energy density in the hadronic phase ( $\varepsilon/T^4 = \pi^2/30 \times 3 \approx 1$ ). Similarly, in SU(2) pure gauge theory it has been noted that a gas of non-interacting glueballs cannot account for the observed energy density below  $T_c$ [11].

In Fig. 9 we also compare the  $N_t = 6$  equation of state with an earlier result on  $N_t = 4$  lattices and with the continuum and lattice Stefan-Boltzmann laws. There is an apparent large finite size effect which is expected from the free lattice theory. At high temperature the energy density has leveled off dramatically while the pressure is still increasing at the largest value of  $T$  that we simulated. Because of asymptotic freedom,  $\varepsilon$  and  $3p$  should approach the Stefan-Boltzmann result for the corresponding value of  $N_t$ . But, from Fig. 9, the approach to the free result is evidently quite slow.

## 4.1 Extrapolation to $m_q = 0$

The above results pertain to unphysical values of the quark mass. Indeed, we would like to obtain the equation of state along a line of constant physics corresponding to the real (two flavor!) world. This can be done by extrapolating to the chiral limit,  $am_q \rightarrow 0$ . To this end we fit the derivatives of the free energy density to an appropriate function of  $6/g^2$  and  $am_q$

and then set  $am_q = 0$ . The fit serves the dual purpose of smoothing the data and allowing a parameterization of the equation of state in terms of the bare quantities, from which we can extract, *e. g.*, the speed of sound.

If the QCD high temperature phase transition with two flavors is a second order transition at zero-quark-mass driven by the restoration of chiral symmetry[12], then the critical part of the free energy should have a universal form, up to the scale of the gauge coupling and quark mass[13]. The free energy is the sum of an analytic piece and a scaling piece:

$$f = f_a(6/g^2, am_q) + f_s(t, h) \quad (13)$$

where  $t = (T - T_c)/T_0$  and  $h = H/H_0$ .  $T_0$  and  $H_0$  are conventionally determined by requiring  $\langle \bar{\psi}\psi \rangle(t = 0, h) = h^{1/\delta}$  and  $\langle \bar{\psi}\psi \rangle(t < 0, h = 0) = (-t)^\beta$ . (In the language of spin models,  $\langle \bar{\psi}\psi \rangle$  is the magnetization and  $\langle \square \rangle$  is the energy.) From invariance under a length rescaling by a factor  $b$ , the critical part of the free energy should have the property:

$$f_s(t, h) = b^{-d} f_s(b^{y_t} t, b^{y_h} h) \quad (14)$$

This implies that the magnetization near the critical point is determined by a universal scaling function, conventionally written as:

$$\frac{M}{h^{1/\delta}} = f(t/h^{1/\beta\delta}) = f(x). \quad (15)$$

The normalization conditions on  $t$  and  $h$  then require that  $f(0) = 1$  and  $f(x) \rightarrow (-x)^\beta$  as  $x \rightarrow -\infty$ . This condition, along with the known values of  $y_h$  and  $y_t$ [14], has been used to compare the behavior in  $\langle \bar{\psi}\psi \rangle$  with that expected from O(4) symmetry[15]. Here we wish to use this theoretical input to guide extrapolation of the free energy to physical light quark mass, which is essentially the same as  $am_q = 0$ . We fit to both a scaling form for O(4) in three dimensions and to the form for mean field theory. We expect the mean field form to be a good approximation when the system is not very near the critical point, and the difference between these two forms gives an idea of the systematic errors in this approach.

Since we calculate both  $\langle \bar{\psi}\psi \rangle$  and  $\langle \square \rangle$  (and their derivatives), we would like to treat them equally in fitting the free energy. Therefore we use a formulation of the scaling free energy which handles the energy and magnetization symmetrically. This has been discussed in Ref.[16], so we just summarize it here.

The scaling ansatz, Eq. 14, tells us that if we specify the singular free energy on the unit circle in the  $t, h$  plane, we have specified it for all  $t, h$ . Thus the scaling part of the free energy density can be written

$$f_s(t, h) = b(t, h)^{-d} g(\theta(t, h)) \quad (16)$$

where  $b$  is the solution to

$$(b^{y_t} t)^2 + (b^{y_h} h)^2 = 1 \quad (17)$$



fit	$6/g_c^2$	$T_0$	$H_0$	$f_{ns}$	$\chi^2/\text{dof}$
O(4)	5.353	0.522	1.51	$3.339\Delta\beta + 2.30\Delta\beta^2 + 0.98\Delta\beta^3$ $+am_q^2(0.41 + 4.3\Delta\beta - 8.3\Delta\beta^2)$	990/91
MF	5.381	0.546	1.22	$3.221\Delta\beta + 0.505\Delta\beta^2 - 0.221\Delta\beta^3$ $+am_q^2(0.63 + 0.7\Delta\beta - 0.6\Delta\beta^2)$	933/91
cold				$0.132\Delta\beta + 2.02\Delta\beta^2 + 3.195\Delta\beta^3 + -1.23\Delta\beta^4$ $+am_q(1.04\Delta\beta + 0.723\Delta\beta^2 + 5.5\Delta\beta^3 - 45\Delta\beta^4)$ $+am_q^2(-1.34\Delta\beta - 12\Delta\beta^2 + 215\Delta\beta^3 + 2.2\Delta\beta^4)$	130/52

Table 1: Fit summary table.  $f_{ns}$  is the non-singular free energy up to an overall constant. Note  $\Delta\beta \equiv 6/g^2 - 5.4$ .

and

$$\theta(t, h) = \tan^{-1}(b^{y_h}h, b^{y_t}t) \quad . \quad (18)$$

Here  $g(\theta)$  is a universal function. In Ref.[16]  $g(\theta)$  for O(4) is determined approximately by Monte Carlo simulation of the O(4) spin model. For this formulation it is convenient to modify the conventional normalizations of  $t$  and  $h$ , and use  $t = (T - T_c)/T_g$  and  $h = H/H_g$ , where  $T_g$  and  $H_g$  are chosen to fix  $g(\pi/2) = y_h/d$  and  $g'(\pi) = -1$ . These are related to the conventional normalizations by  $H_0 = H_g^{\delta+1}$  and  $T_0 = T_g H_g^{1/\beta}$ .

From simulation of the O(4) spin model an approximate  $g(\theta)$  for O(4)[16] has been obtained. For the mean field case, the scaling function can be obtained from a numerical re-parameterization of the mean field magnetic equation of state[13]

$$h/M^3 = 1 + t/M^2 \quad . \quad (19)$$

Fig. 4 shows  $\langle\bar{\psi}\psi\rangle$  calculated from fits to the mean field and O(4) scaling functions, plus polynomials in  $am_q$  and  $6/g^2$ . We also include the pure polynomial fit to the cold data, and both hot and cold data are shown for comparison. The fits are summarized in Table 1.  $\chi^2$  per degree of freedom is poor for all of the fits. For the hot data, the mean field and O(4) cases each have  $\chi^2/\text{dof} \approx 1000/91$  while the cold data has  $\chi^2/\text{dof} \approx 130/52$ . If we fit to the data without step size extrapolations, the results improve somewhat,  $\chi^2/\text{dof} \approx 650/91$  for the hot data and  $117/56$  for the cold. A fit to only  $\langle\bar{\psi}\psi\rangle$  over the same range gives  $\chi^2/\text{dof} \approx 49/18$ . Despite the high  $\chi^2$ , examination of Fig. 4 shows that the data are actually reproduced quite well by the fits. This is remarkable given the large range of  $am_q$  and  $6/g^2$  spanned by the fits. Moreover, the fits to mean field and O(4) scaling functions work equally well; our data cannot distinguish between the two scaling behaviors. However, it is interesting to note that the respective extrapolations to  $m_q = 0$  are quite different, and give critical temperatures  $T_c \approx 140$  and  $150$  MeV for O(4) and mean field respectively. The above indicates that the present lattice simulations may still be too far from the scaling region and smaller quark masses are required to see the true scaling behavior. The correlation length in lattice units

as given by the inverse pion mass (the pion and sigma are degenerate at the critical point) of the present simulations is only 2-3 which is less than the temporal extent of the lattice, so true dimensional reduction, which must occur for universality arguments to hold, has not been achieved.

At  $am_q = 0$ ,  $\partial(am_q)/\partial(\log a) = 0$  so the interaction measure is determined solely from the plaquette. However, most of our information about the critical behavior comes from  $\langle\bar{\psi}\psi\rangle$ , since the contribution of the scaling part of the free energy to the plaquette is small compared with the analytic part. Therefore in a crude approximation our procedure is using information about  $\langle\bar{\psi}\psi\rangle$  to help determine the free energy, which in turn yields the plaquette as  $am_q \rightarrow 0$ .

An extrapolation of the equation of state to  $m_q = 0$  is shown in Fig. 10. It is compared to the  $am_q = 0.0125$  result which reproduces the data reasonably well. The appearance of the bump in the energy density just after the transition is probably an artifact of the extrapolation (at  $m_q = 0$ , the corresponding region of  $6/g^2$  lies below the values of the coupling where we have done simulations). From Fig. 10 we again see a weak dependence on the quark mass, which gives us some reassurance in the extrapolation. The plus and minus one standard deviations shown in Fig. 10 are calculated in the following way. First, we do a covariant fit to  $\langle\Box\rangle$ ,  $\langle\bar{\psi}\psi\rangle$ , and their derivatives with respect to  $6/g^2$  (Eqs. 5-8). From the fit we obtain a set of parameters and the covariances of these parameters which map onto a multi-dimensional Gaussian probability distribution for the parameters. We then generate many parameter sets with this distribution and calculate the equation of state for each one. The standard deviation of the mean of this set is shown in the figure.

In Fig. 11 we show the speed of sound squared calculated from the O(4) fit. It rises rapidly through the transition region and then levels off near the free value of  $1/3$ . This indicates that the system is weakly interacting in this region. This should be contrasted with  $\varepsilon - 3p$  just after the crossover which indicates significant interaction effects. Indeed, the couplings in the region are of order one, and we have already seen that neither the energy density nor pressure is approaching its perturbative value. The low temperature part of the curve is probably not accurate. The derivatives of the energy density and pressure are poorly known in this region since the difference of  $\langle\Box\rangle$  and  $\langle\bar{\psi}\psi\rangle$  from their cold lattice values is nearly zero. We have already mentioned that  $m_\pi/T_c$  was rather high in our simulations, so it is not surprising that the expected dynamics of a dilute gas of relativistic pions is not observable. In that case, we expect the hadron gas below the transition to have a nonzero speed of sound, which then dips down at the transition. The statistical errors for the speed of sound were calculated in the same manner described above for the equation of state.

## 5 Conclusions

In this work we have pushed our calculation of the equation of state for QCD including dynamical quarks to smaller lattice spacing. We have also developed techniques for using theoretical expectations for the scaling behavior to extrapolate numerical results to the physical quark mass. The points where we ran were chosen to explore the equation of state over a range of temperature rather than to work very close to the crossover. Therefore, we can say little about the nature of the transition or crossover from this work. Still, our results are consistent with the standard picture of a second order phase transition at zero-quark-mass and a sharp crossover for small but nonzero masses.

We remark, however, that recent simulations with two flavors of Kogut-Susskind quarks on lattices with  $N_t = 4$  and at smaller quark masses than used in this study have revealed significant finite size effects that have cast doubt on earlier promising demonstrations of critical scaling[17]. Other recent simulations with two flavors of Wilson quarks and an improved gauge action to reduce cutoff effects also show promising agreement with  $O(4)$  scaling, but a thorough investigation of finite-size effects remains to be done[18]. So for the moment the question of the order and universality class of the transition remains open, and the validity of our extrapolation to zero quark mass remains to be established. At the very least, one may expect that the recently reported finite volume corrections lead to a greater sharpening of the crossover in energy density and speed of sound as the quark mass is decreased. We have seen that small changes in the extrapolation have a large effect on some but not all extrapolated values: *e.g.*  $O(4)$  and mean-field extrapolations give zero-quark-mass critical temperatures that differ by 10 MeV. On the other hand, expressed as a function of temperature in physical units, the energy density and pressure away from the crossover show little dependence on quark mass, even in the zero-quark-mass limit.

The methods used here require a subtraction of the zero temperature plaquette and  $\langle\bar{\psi}\psi\rangle$ . As  $N_t$  is increased, the plaquette subtraction rapidly becomes more difficult, since the fractional difference in plaquette between the hot and cold lattices decreases as  $N_t^{-4}$ . This suggests that, as for many other quantities, an improved action which allows use of a larger lattice spacing, or smaller  $N_t$ , will be important for further progress. Results for pure gauge theory and for four-flavor QCD have been reported by the Bielefeld group[19]. Another important problem for future studies is remedying the breaking of flavor symmetry, so that the low temperature phase that is simulated really has three light pions. For a start in this direction see Ref.[2].

### Acknowledgments

This work was supported by NSF grants NSF-PHY93-09458, NSF-PHY96-01227, NSF-PHY91-16964, DOE contracts DE-AC02-76CH-0016, DE-AC02-86ER-40253, DE-FG03-

95ER-40906, DE-FG05-85ER250000, DE-FG05-92ER40742, and DOE grants DE-2FG02-91ER-40628, DE-FG02-91ER-40661. Calculations were carried out on the following: the Intel Paragon at the San Diego Supercomputer Center, the Intel Paragon at Indiana University, the IBM SP2 at the Cornell Theory Center, the IBM SP2 at the University of Utah, and the workstation cluster at SCRI.

## References

- [1] For example, see D.H. Rischke, M. Gyulassy, “The Time-Delay Signature of Quark-Gluon-Plasma Formation in Relativistic Nuclear Collisions”, nucl-th/9606039.
- [2] T. Blum, C. DeTar, S. Gottlieb, U.M. Heller, J.E. Hetrick, K. Rummukainen, R. L. Sugar, D. Toussaint, M. Wingate “Improving flavor symmetry in the Kogut-Susskind hadron spectrum”, hep-lat/9609036, to appear in Phys. Rev. D. It may be possible to effectively eliminate flavor symmetry breaking in lattice simulations altogether. See T. Blum and A. Soni, “QCD with domain wall quarks”, hep-lat/9611030, and references therein.
- [3] Preliminary results were reported in C. Bernard, T. Blum, C.E. DeTar, S. Gottlieb, U.M. Heller, J. E. Hetrick, L. Kärkkäinen, C. McNeile, K. Rummukainen, R. L. Sugar, D. Toussaint, M. Wingate, hep-lat/9608026, to be published in Nuc. Phys. B[Proc. Suppl.].
- [4] T. Blum, S. Gottlieb, L. Kärkkäinen, and D. Toussaint, Nucl. Phys. B (Proc. Suppl.) **42**, 460 (1995); Phys. Rev. D. **51** (1995) 5153.
- [5] F. Karsch, Nucl. Phys. **B205**, 285 (1982).
- [6] S. Huang, J. Potvin, C. Rebbi and S. Sanielevici, Phys. Rev. D **42**, 2864 (1990).
- [7] J. Engels, J. Fingberg, F. Karsch, D. Miller and M. Weber, Phys. Lett. B **525**, 625 (1990). J. Engels, F. Karsch, K. Redlich, Nucl. Phys. **B435**, 295 (1995).
- [8] S. Gottlieb, W. Liu, R. L. Renken, R. L. Sugar and D. Toussaint, Phys. Rev. D **35**, 2531 (1987).
- [9] C. Bernard, T. Blum, C. DeTar, S. Gottlieb, K. Rummukainen, U.M. Heller, J. Hetrick, D. Toussaint, and R. L. Sugar, Phys. Rev. D **54** 4585 (1996), and references therein.
- [10] The energy density in the SU(3) pure gauge case is also substantial below  $T_c$  (F. Karsch, private communication). For the critical temperature of the SU(3) pure gauge transition see : G. Boyd, J. Engels, F. Karsch, E. Laermann, C. Legeland, M. Luetgemeier, B. Petersson, Nucl. Phys. **B469**, 419 (1996). Lattice estimates of the mass of the lightest

- glueball have been given in G. Bali, K. Schilling, A. Hulsebos, A. Irving, C. Michael, and P. Stephenson, Phys. Lett. B **309**, 378 (1993); H. Chen, J. Sexton, A. Vaccarino, and D. Weingarten, Nucl. Phys. B (Proc. Suppl.) **34**, 357 (1994); and J. Sexton, A. Vaccarino, and D. Weingarten, Phys. Rev. Lett. **75** (1995) 4563.
- [11] J. Engels, F. Karsch, and K. Redlich, Nucl. Phys. **B435**, 295 (1995).
  - [12] R.D. Pisarski and F. Wilczek, Phys. Rev. D **29** (1984) 338; F. Wilczek, J. Mod. Phys. **A7**, 3911 (1992); K. Rajagopal and F. Wilczek, Nucl. Phys. B**399** (1993) 395; K. Rajagopal, in *Quark Gluon Plasma 2*, R. Hwa, ed. (World Scientific, Singapore, 1995).
  - [13] D.J. Amit, *Field Theory, the Renormalization Group, and Critical Phenomena*, (McGraw-Hill, New York, 1978); P. Pfeuty and G. Toulouse, *Introduction to the renormalization group and its applications*, (Wiley, New York, 1977).
  - [14] G. Baker, D. Meiron and B. Nickel, Phys. Rev. B **17**, 1365 (1978); K. Kanaya and S. Kaya, Phys. Rev. D **51**, 2404 (1995); P. Butera and M. Comi, Phys. Rev. B **52**, 6185 (1995).
  - [15] F. Karsch and E. Laermann, Phys. Rev. D **50**, 6954 (1994). F. Karsch, [hep-lat/9503010](#), review talk from “Quark Matter 95”; C. DeTar, Nucl. Phys. B (Proc. Suppl.) **42**, 73 (1995); G. Boyd, J. Engels, F. Karsch, E. Laermann, C. Legeland, M. Lütgemeier, and B. Petersson, Phys. Rev. Lett. **75**, 4169 (1995).
  - [16] D. Toussaint, [hep-lat/9607084](#), to be published in Phys. Rev. D.
  - [17] Problems with O(4) scaling were reported by A. Ukawa at the XIVth International Symposium on Lattice Field Theory, June 4-8th, 1996, St. Louis, to appear in Nucl. Phys. B (Proc. Suppl.), [hep-lat/9612011](#); G. Boyd reported similar findings by the Bielefeld group, “Two flavour QCD phase transition”, [hep-lat/9607046](#); We are currently carrying out simulations at  $N_t = 4$  with  $am_q = 0.008 - .025$  on lattices with spatial sites  $12^3$ ,  $16^3$ , and  $24^3$ . Our preliminary results are consistent with the above.
  - [18] Y. Iwasaki, K. Kanaya, S. Kaya, T. Yoshie, “Scaling of the chiral order parameter in two-flavor QCD”, [hep-lat/9609022](#).
  - [19] F. Karsch, B. Beinlich, J. Engels, R. Joswig, E. Laermann, A. Peikert, B. Petersson, “QCD Thermodynamics with Improved Actions”, [hep-lat/9608047](#).

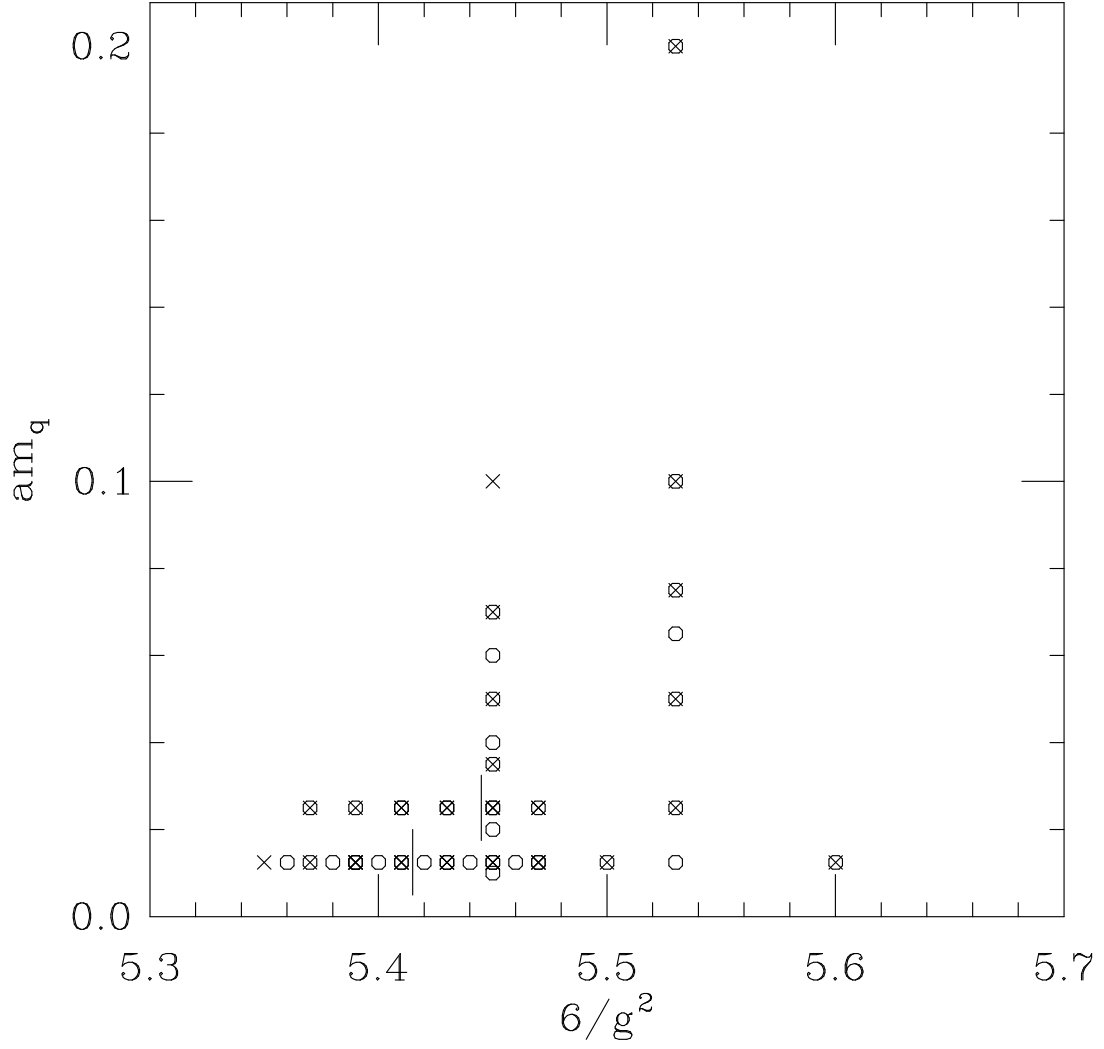


Figure 1: Phase diagram for our simulations. The vertical solid lines indicate approximate locations of the crossover. Crosses indicate cold lattices, octagons hot lattices.

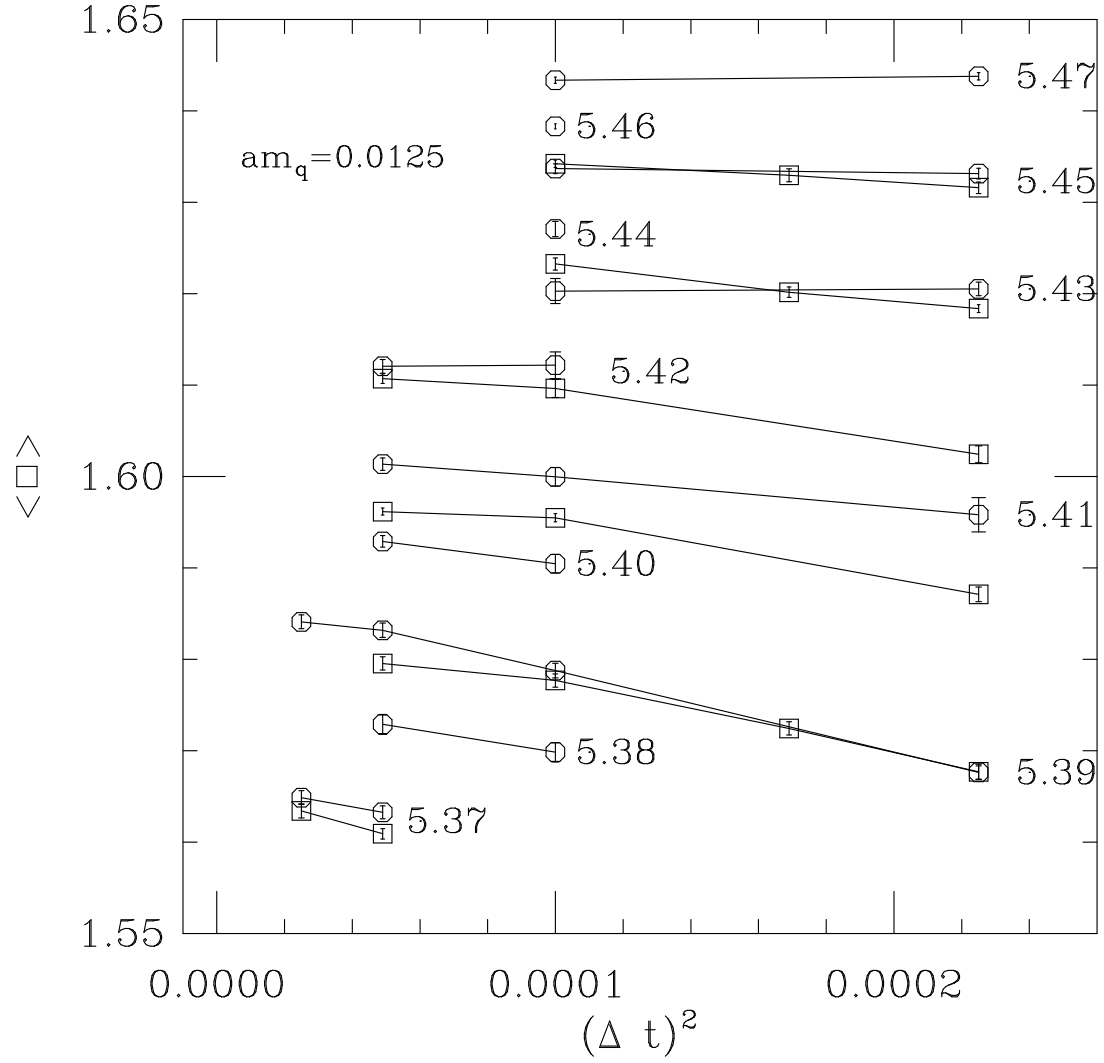


Figure 2: The plaquette expectation value as a function of the step size squared,  $\Delta t^2$ , and the gauge coupling. Results are shown for  $am_q = 0.0125$ . Octagons denote hot lattices ( $6/g^2$  is given for each) and squares denote cold lattices.

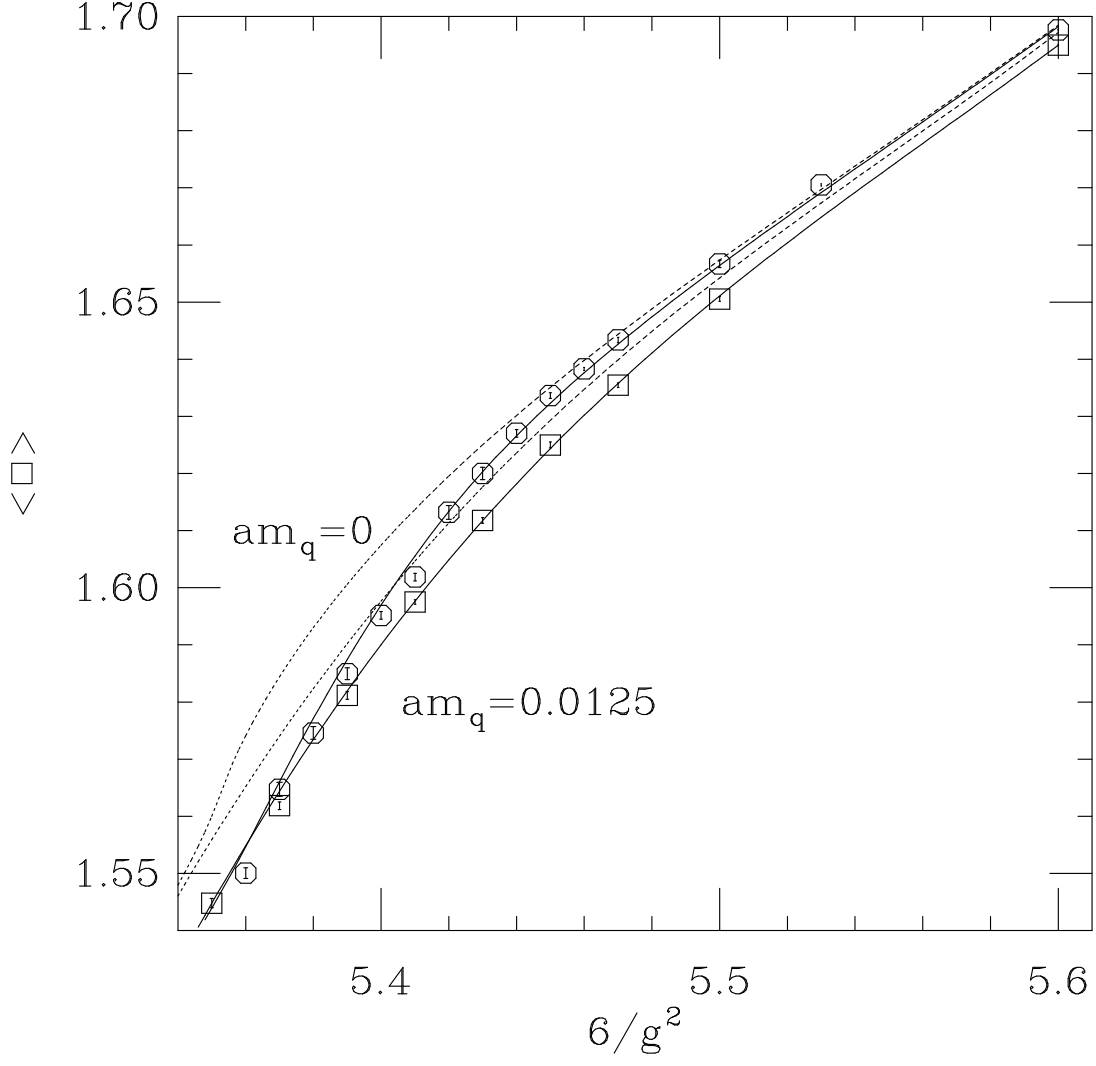


Figure 3: The plaquette expectation value as a function of the gauge coupling at  $am_q = 0.0125$ . Octagons denote hot lattices, squares cold lattices. The area between the curves gives the pressure while the difference at each point is related to the interaction measure. The lines are from a fit including the  $O(4)$  singular free energy described in the text (dashed lines are an extrapolation to  $am_q = 0$ ).



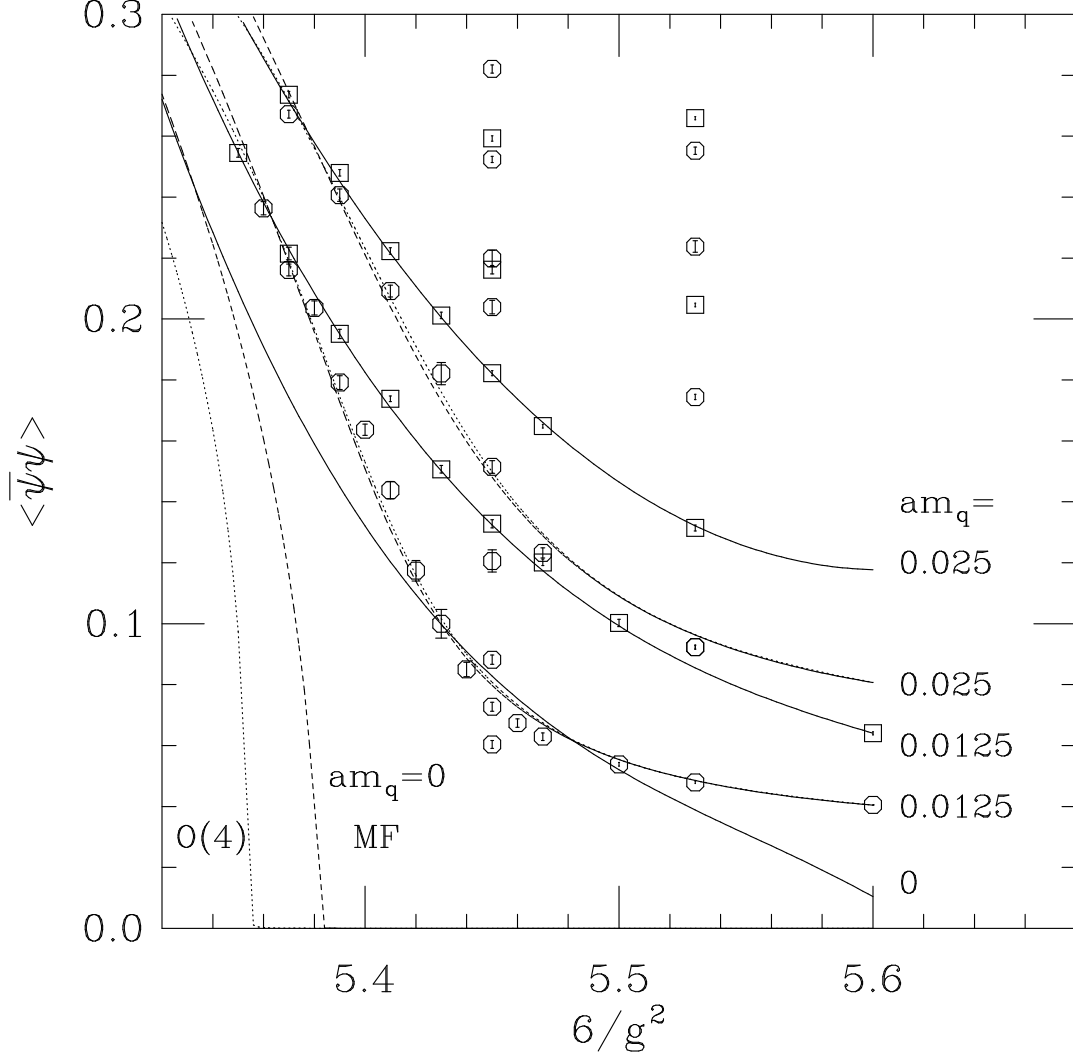


Figure 4:  $\langle \bar{\psi}\psi \rangle$  as a function of  $6/g^2$  and  $am_q$ . The difference in the hot (octagons) and cold (squares) values is related to the interaction measure.  $\langle \bar{\psi}\psi \rangle$  on the hot lattices also serves as an order parameter for the system. Lines depict fits to O(4) and mean field singular forms of the free energy plus analytic terms to  $\langle \square \rangle$ ,  $\langle \bar{\psi}\psi \rangle$ , and their derivatives (Eqs. 5-8). Only points with  $am_q \leq 0.025$  were included in the fits. The difference between O(4) (dotted line) and mean field forms (dashed line) is not discernible at the quark masses where simulations were run. Extrapolations to  $m_q = 0$ , however, give different critical couplings. Solid lines correspond to polynomial fits to the cold data and the corresponding extrapolation to  $am_q = 0$ .

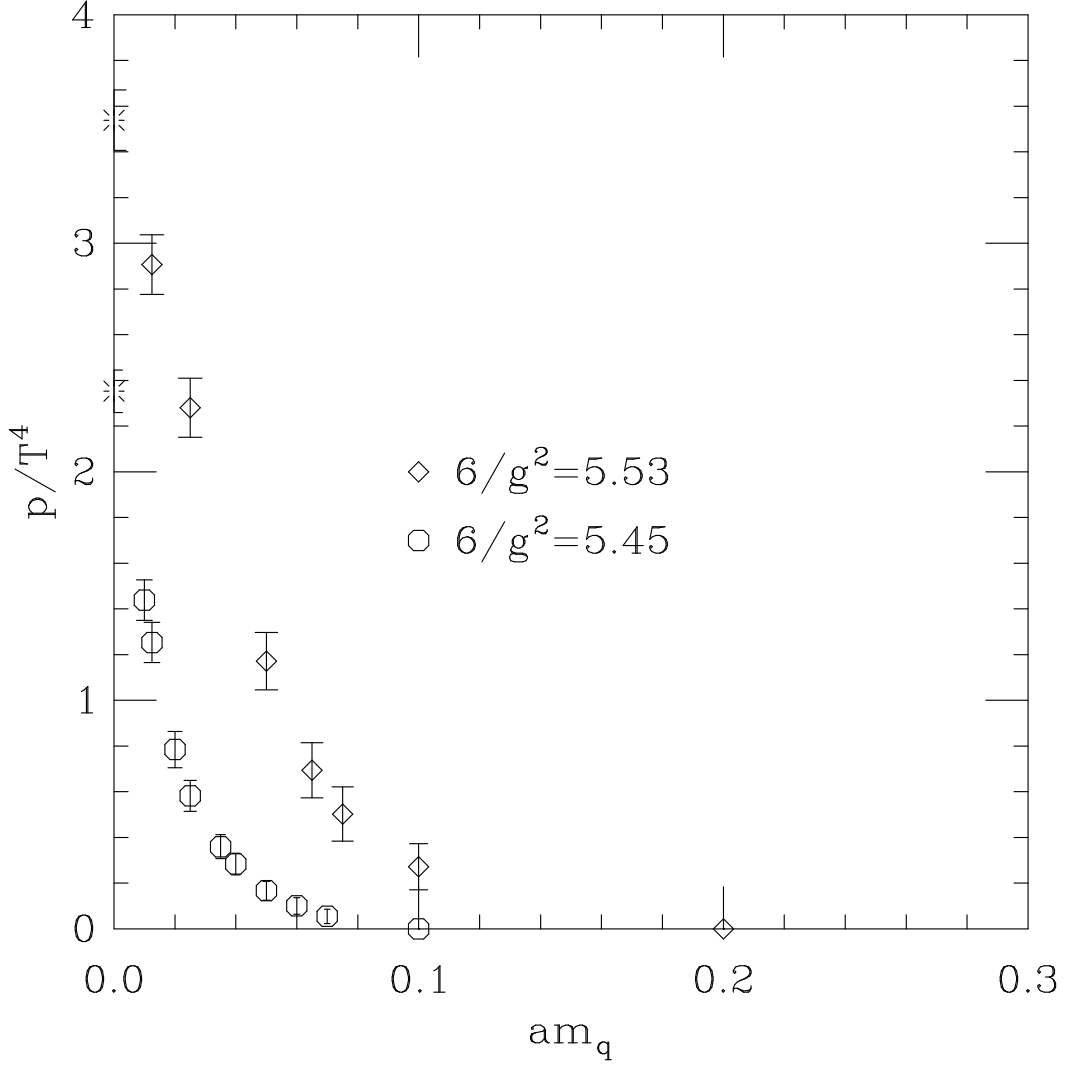


Figure 5: The pressure obtained from integrating  $\langle \bar{\psi}\psi \rangle$  with respect to  $am_q$  and constant  $6/g^2$ . The values at zero-quark-mass (bursts) are obtained by setting  $\langle \bar{\psi}\psi \rangle = 0$  on the hot lattices and extrapolating  $\langle \bar{\psi}\psi \rangle$  to  $am_q = 0$  on the cold lattices.

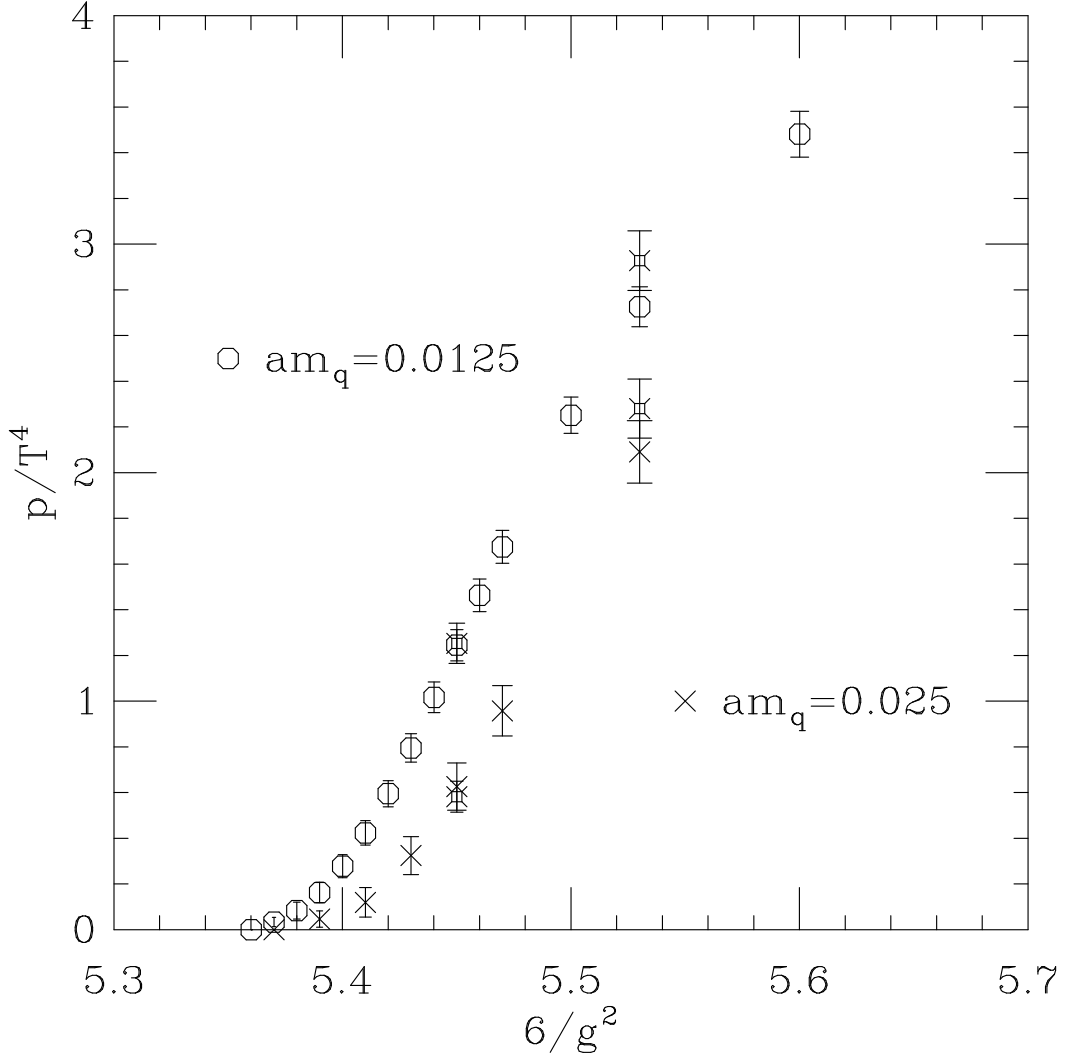


Figure 6: The pressure obtained from integrating  $\langle \square \rangle$  with respect to  $6/g^2$  at constant  $am_q$ . The values from the quark mass integrations (fancy squares) are also shown for comparison.

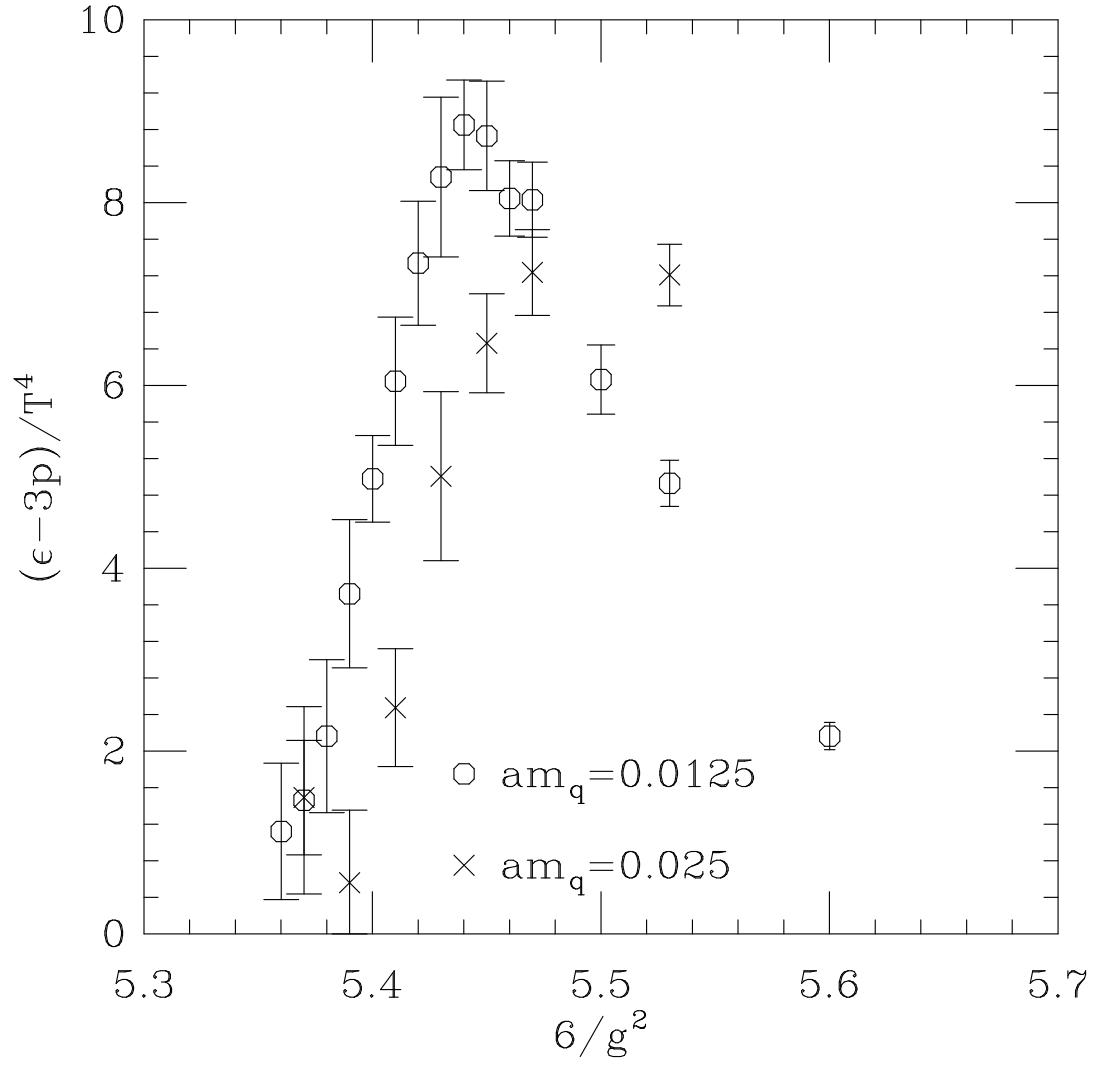


Figure 7: The interaction measure,  $\epsilon - 3p$ .

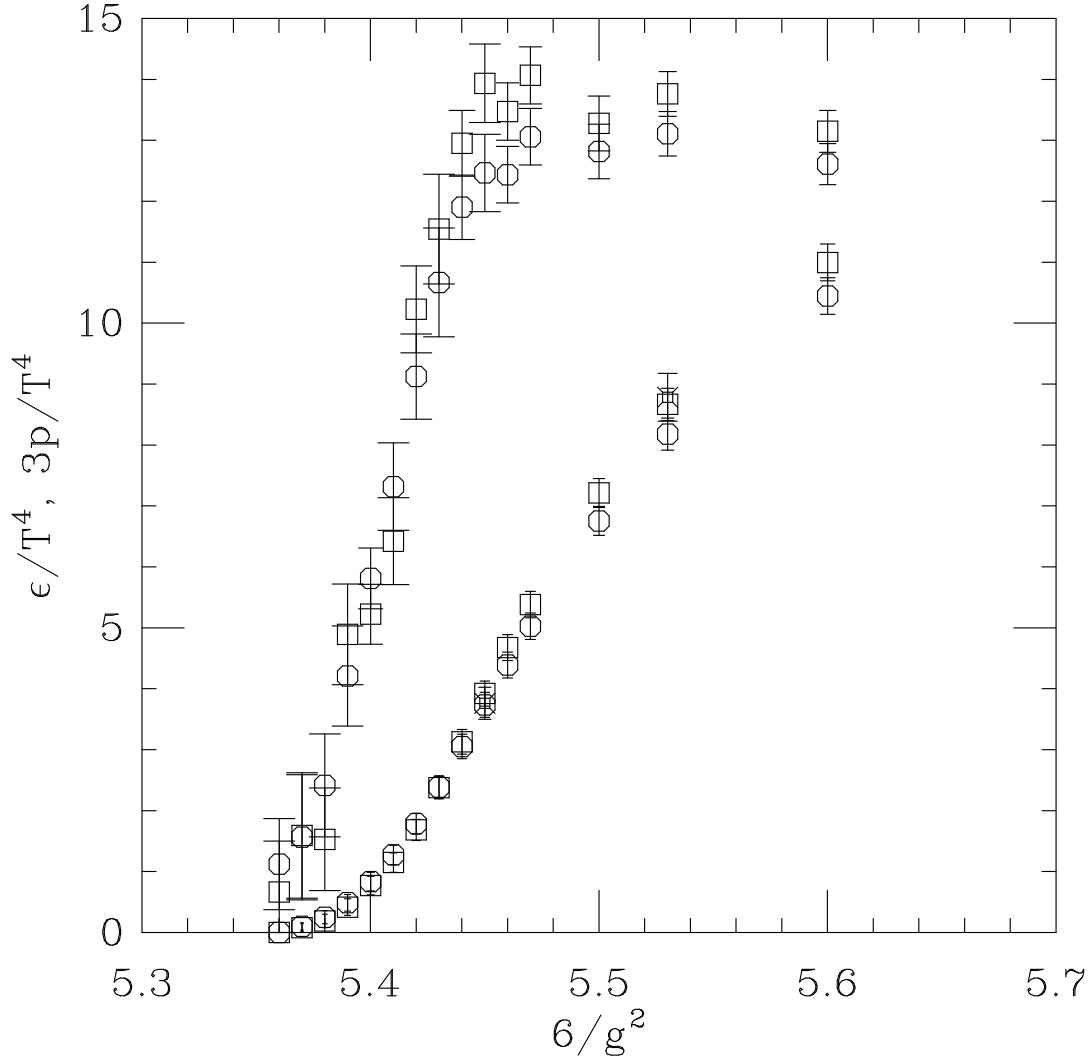


Figure 8: The energy density constructed from  $I + 3p$  (upper two curves). Also shown is  $3p$  (lower two curves) and results with no step size extrapolations (squares). The difference is the step size systematic error in the equation of state. The data are for  $am_q = 0.0125$  only. The fancy squares denote 3 times the pressure as calculated from the integration of  $\langle \bar{\psi}\psi \rangle$  with respect to  $am_q$ .

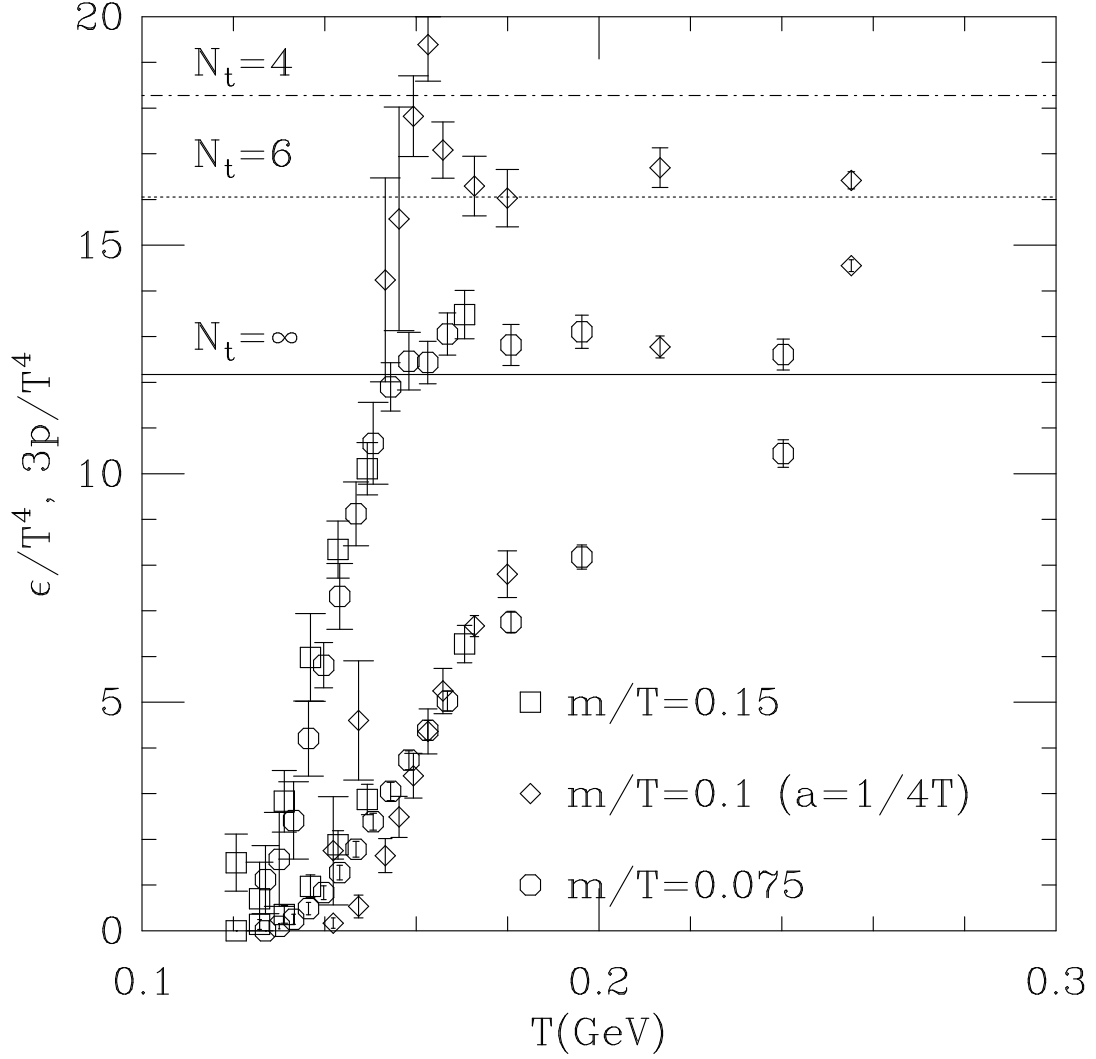


Figure 9: The equation of state along lines of constant  $m_q/T$ . The octagons denote  $am_q = 0.0125$  results, squares  $am_q = 0.025$ . The diamonds indicate an earlier result on  $N_t = 4$  lattices. Horizontal lines correspond to Stefan-Boltzmann laws for  $N_t = 4, 6$ , and the continuum. The energy density increases rapidly near the crossover while the pressure (lower curve for each symbol) rises smoothly.

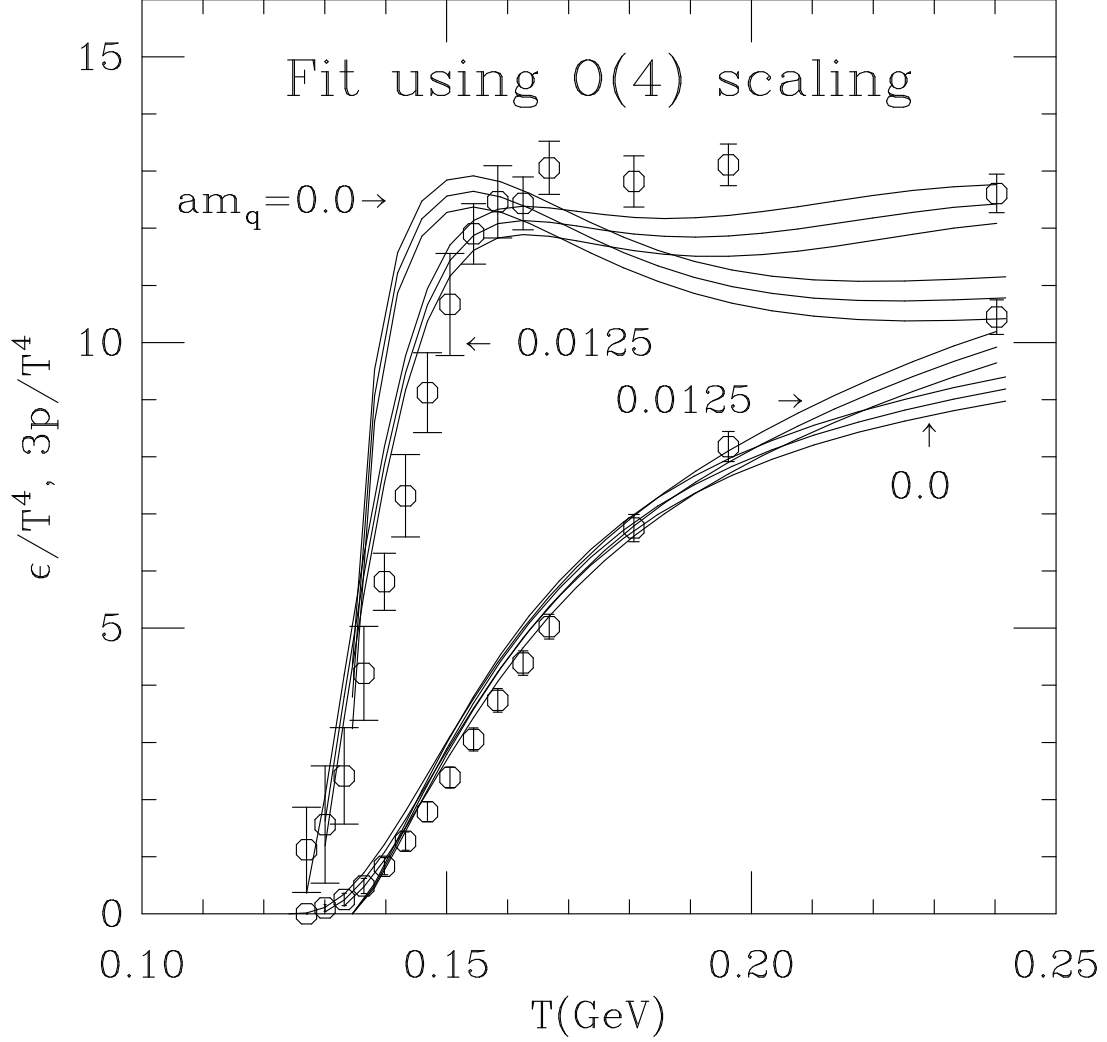


Figure 10: The  $am_q = 0$  equation of state from a fit to the data that includes the O(4) universal scaling function. Also shown is the data and the fit at  $am_q = 0.0125$  for comparison. Again, there is only a weak mass dependence. The “bump” just after the transition is likely an artifact of the extrapolation. The solid lines correspond to the central value and a one standard deviation above and below this result (statistical errors only).

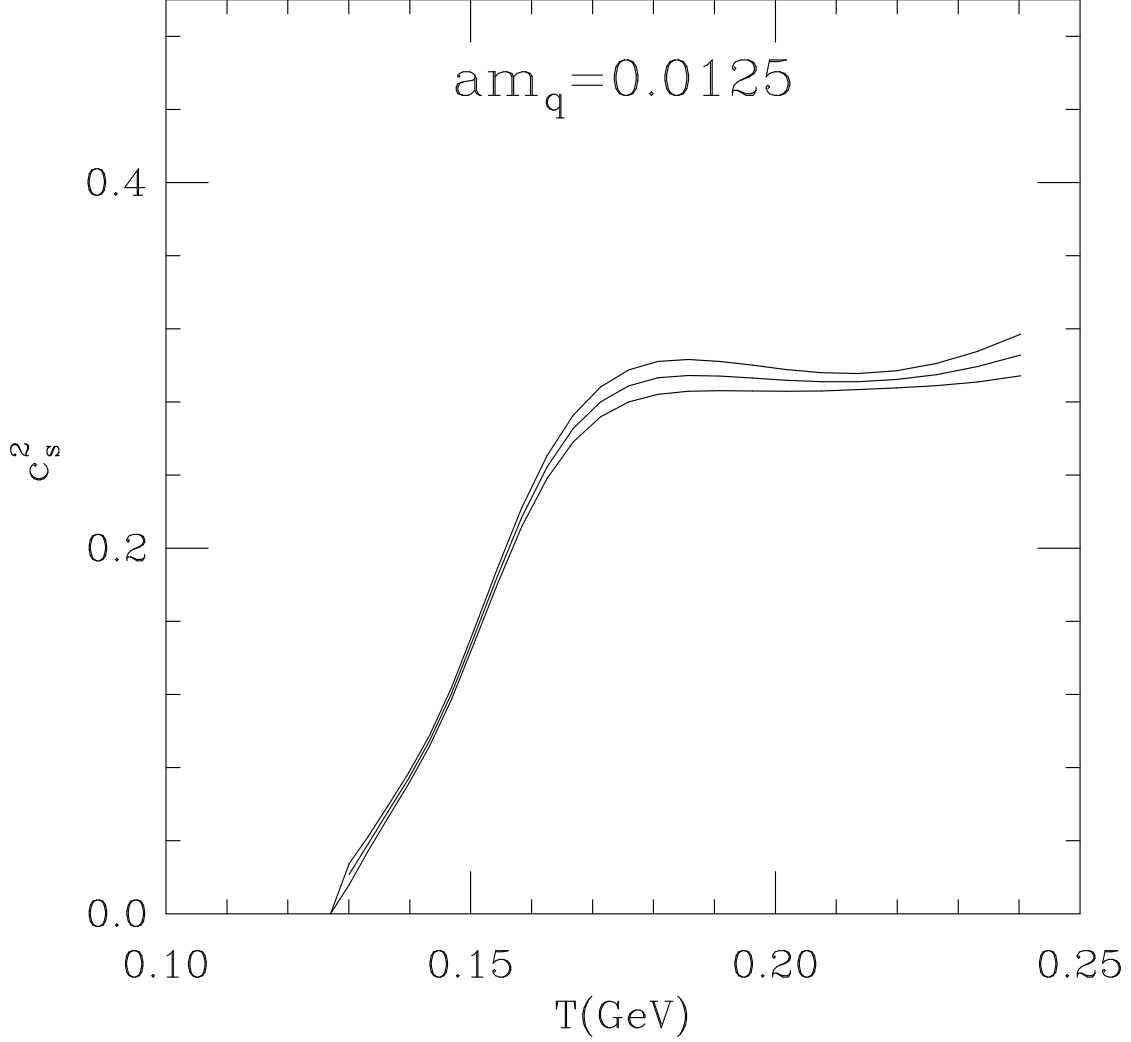


Figure 11: The speed of sound squared from a fit to the data that includes the O(4) universal scaling function.  $c_s^2$  rises rapidly in the crossover region and then approaches the free gas result,  $1/3$ . The low temperature result is probably not accurate (see text). The solid lines correspond to the central value and a one standard deviation above and below this result (statistical errors only).